

A Preliminary Survey of Radio-Frequency Interference Over the U.S. in Aqua AMSR-E Data

Li Li, *Member, IEEE*, Eni G. Njoku, *Fellow, IEEE*, Eastwood Im, *Senior Member, IEEE*, Paul S. Chang, *Senior Member, IEEE*, and Karen St. Germain, *Senior Member, IEEE*

Abstract—A spectral difference method is used to quantify the magnitude and extent of radio-frequency interference (RFI) observed over the United States in the Aqua AMSR-E radiometer channels. A survey using data from the AMSR-E instrument launched in May 2002 shows the interference to be widespread in the C-band (6.9 GHz) channels. The RFI is located mostly, but not always, near large highly populated urban areas. The locations of interference are persistent in time, but the magnitudes show temporal and directional variability. Strong and moderate RFI can be identified relatively easily using an RFI index derived from the spectral difference between the 6.9- and 10.7-GHz channels. Weak RFI is difficult to distinguish, however, from natural geophysical variability. These findings have implications for future microwave sensing at C-band, particularly over land areas. An innovative concept for radiometer system design is also discussed as a possible mitigation approach.

Index Terms—Advanced Microwave Scanning Radiometer (AMSR), microwave radiometry, radio-frequency interference (RFI), land remote sensing.

I. INTRODUCTION

THE ADVANCED Microwave Scanning Radiometer (AMSR-E) [1] was developed by the National Space Development Agency of Japan (NASDA) and launched onboard the National Aeronautics and Space Administration (NASA) EOS Aqua satellite on May 4, 2002. A sister instrument, the AMSR [2] on the Japanese ADEOS-II satellite, was launched in December 2002. The Naval Research Laboratory's WindSat radiometer [3] on the Coriolis satellite was launched in January 2003. The AMSR's and WindSat are functionally quite similar in terms of frequencies, viewing configurations, and spatial resolutions to the Conical Microwave Imager/Sounder (CMIS) [4] planned for launch as part of the National Polar-orbiting Operational Environmental Satellite System (NPOESS) in the 2008–2009 time frame. All these sensors have dual-polarized

Manuscript received December 18, 2002; revised April 7, 2003. This research was supported jointly by the Earth Observing System (EOS) Aqua Algorithm and Validation Program of NASA, and by the NOAA NPOESS Integrated Program Office (IPO) under contract with NOAA/NESDIS/ORA. This research was carried out in part at the Jet Propulsion Laboratory, California Institute of Technology, under contract with the National Aeronautics and Space Administration.

L. Li, E. G. Njoku, and E. Im are with the Jet Propulsion Laboratory, California Institute of Technology, Pasadena, CA 91109 USA (e-mail: li.li@jpl.nasa.gov; eni.g.njoku@jpl.nasa.gov; eastwood.im@jpl.nasa.gov).

P. S. Chang is with the Office of Research and Applications, National Environmental Satellite, Data and Information Service, National Oceanic and Atmospheric Administration, Camp Springs, MD 20746 USA (e-mail: paul.s.chang@noaa.gov).

K. M. St. Germain is with the Remote Sensing Division, Naval Research Laboratory, Washington, DC 20375 USA (e-mail: karen.Stgermain@nrl.navy.mil).

Digital Object Identifier 10.1109/TGRS.2003.817195

TABLE I
AMSR-E CHARACTERISTICS

Frequency (GHz)	6.925	10.65	18.7	23.8	36.5	89.0
Bandwidth (MHz)	350	100	200	400	1000	3000
Sensitivity (K)	0.3	0.6	0.6	0.6	0.6	1.1
Instantaneous FOV (km)	75x43	48x27	27x16	31x18	14x8	6x4
Sampling interval (km)	10x10	10x10	10x10	10x10	10x10	5x5
Integration time (msec)	2.6	2.6	2.6	2.6	2.6	1.3
Main beam efficiency (%)	95.3	95.0	96.3	96.4	95.3	96.0
Beamwidth (degrees)	2.2	1.4	0.8	0.9	0.4	0.18

channels near 6.9, 10.8, and 18.7 GHz for ocean and land surface sensing applications. Analyses of data from the AMSR-E, AMSR, and WindSat sensors will provide opportunities for evaluating the CMIS design and expected performance.

Early examinations of AMSR-E instrument data have shown evidence of extensive radio-frequency interference (RFI) in the 6.9-GHz brightness temperature measurements. As part of the evaluation team activities, this paper provides a preliminary analysis of the magnitude and extent of the interference. Our primary objective is to identify, survey, and quantify the RFI, globally and in regions where the problem appears most severe such as the United States. The study results will provide useful information on the utility of the 6.9-GHz channels of AMSR-E, AMSR, and WindSat data for land surface studies (in particular, for soil moisture sensing) and will indicate potential problems and directions for improvement in the future CMIS radiometer.

II. AMSR-E DESCRIPTION

The AMSR-E instrument, developed by NASDA, follows the heritage of spaceborne imaging radiometers including the Scanning Multichannel Microwave Radiometer (SMMR) [5], the Special Sensor Microwave/Imager (SSM/I) [6], and the Tropical Rainfall Measuring Mission (TRMM) Microwave Imager (TMI) [7]. AMSR-E makes dual-polarized passive microwave measurements at six frequencies: 6.9, 10.7, 18.7, 36.5, and 89 GHz. From the 705-km Aqua orbit, the antenna nadir angle of 47.4° provides an earth incidence angle of 55° . The antenna beams scan conically about the nadir axis. The $\pm 61^\circ$ active portion of the azimuth scan angle provides an observation swath width of 1445 km. The orbit is sun-synchronous with equator crossings at 1:30 P.M. and 1:30 A.M. local

TABLE II
RF ALLOCATION

Frequency (GHz)	United States	International	Remarks
6.7–7.2	FIXED FIXED-SATELLITE (Earth-to-space) MOBILE SPACE RESEARCH (Earth-to-space)	FIXED FIXED-SATELLITE (Earth-to-space, Space-to-Earth) MOBILE	Auxiliary Broadcasting Cable TV Relay
10.6–10.7	EARTH EXPLORATION- SATELLITE (passive) SPACE RESEARCH (passive) RADIO ASTRONOMY	EARTH EXPLORATION- SATELLITE (passive) SPACE RESEARCH (passive) RADIO ASTRONOMY MOBILE	Fixed Microwave
18.6–18.8	EARTH EXPLORATION- SATELLITE (passive) FIXED-SATELLITE (Earth-to-space) SPACE RESEARCH (passive)	EARTH EXPLORATION- SATELLITE (passive) FIXED-SATELLITE (space-to- Earth) FIXED MOBILE	Satellite Communication
23.6–24.0	EARTH EXPLORATION- SATELLITE (passive) RADIO ASTRONOMY SPACE RESEARCH (passive)	EARTH EXPLORATION- SATELLITE (passive) RADIO ASTRONOMY	
36.0–37.0	EARTH EXPLORATION- SATELLITE (passive) SPACE RESEARCH (passive) FIXED MOBILE	EARTH EXPLORATION- SATELLITE (passive) SPACE RESEARCH (passive) FIXED MOBILE	
86.0–92.0	EARTH EXPLORATION- SATELLITE (passive) RADIO ASTRONOMY SPACE RESEARCH (passive)	EARTH EXPLORATION- SATELLITE (passive) RADIO ASTRONOMY SPACE RESEARCH (passive)	

solar time. Additional details of the radiometer and antenna characteristics are listed in Table I.

The AMSR-E Level 1A data are generated at the NASDA Earth Observation Center (EOC) in Japan. The Level 1A data contain sensor counts and coefficients needed to compute antenna temperatures and, subsequently, surface brightness temperatures at level 1B. The level 1A data are sent to the Physical Oceanography Distributed Active Archive Center (PO.DAAC) located at the Jet Propulsion Laboratory in Pasadena, CA. From there, the data are transmitted to the AMSR-E Science Information Processing System (SIPS) in the United States. The SIPS has two components, one located at the Remote Sensing Systems (RSS) facility in Santa Rosa, CA, and the other at the Global Hydrology and Climate Center (GHCC) in Huntsville, AL. At the RSS SIPS, Level 2A brightness temperatures are generated by reconstructing the AMSR-E antenna gain patterns at each channel to five footprints, corresponding to the footprint sizes of the 6.9-, 10.7-, 18.7-, 36.5-, and 89-GHz observations (see [8] and <http://www.ghcc.msfc.nasa.gov/AMSR/>). The sampling intervals are approximately 10 km for the four low resolutions, and 5 km for the highest resolutions. The level 2A data contain as a subset the level 1B data. The Level 2A data are sent to the GHCC SIPS for higher level processing. The data products are subsequently transferred to the National Snow and Ice Data Center (NSIDC) DAAC in Boulder, CO for archiving and distribution.

III. RFI AND NATURAL EMISSION CHARACTERISTICS

Microwave radiometers are sensitive devices designed to measure relatively weak naturally emitted thermal radiation

over broad spectral bands. Man-made emissions from active microwave transmitters are distinctly different than those of natural sources in terms of intensity, spatial variability, polarization, and spectral characteristics. Although typically narrowband, these signals have high power levels that can cause spurious measurements and saturate a radiometer receiver if the transmissions fall within its measurement frequency band. From a radiometric point of view, these interfering sources are classed as radio-frequency interference. RFI signals typically originate from coherent point targets, i.e., radiating devices and antennas. Their power levels are several orders of magnitude higher than natural thermal emissions and are often directional and can be either continuous or intermittent. RFI originates from a wide variety of sources, typically clustered near highly populated areas and centers of technical and industrial activity.

The World Radiocommunication Conferences recommend allocations of the RF spectrum for various services, including passive services such as passive earth exploration satellites and radio astronomy. These allocations are documented internationally by the Radio Regulations of the International Telecommunications Union [9]. Within the United States, the Office of Spectrum Management of the National Telecommunications and Information Administration (NTIA) has responsibility for spectrum management. Table II shows the spectrum allocations at the AMSR-E frequencies as listed by the NTIA (<http://www.ntia.doc.gov/osmhome/red-book/redbook.html>). Near 7 GHz, the “Fixed” and “Mobile” radio services, including cable television relay and auxiliary broadcasting, are the major sources of RFI for spaceborne radiometry. The actual sources and characteristics of RFI can

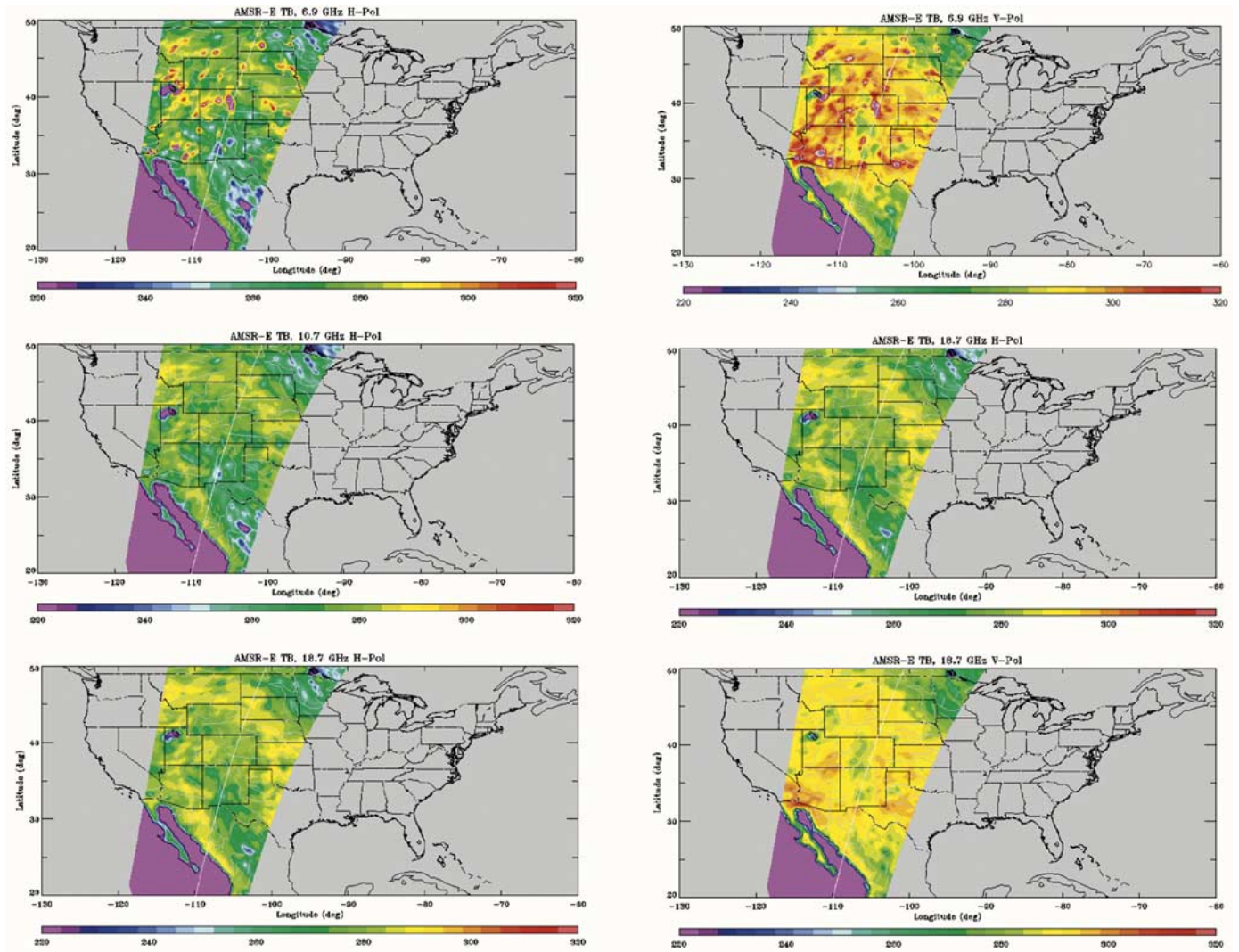


Fig. 1. AMSR-E brightness temperatures at 6.9, 10.6, and 18.7 GHz, horizontal and vertical polarizations, over the United States.

only be determined by measuring the radio spectrum in this frequency band at the RFI contamination sites.

Natural radiation emitted by the earth's surface and atmosphere has characteristics that are very different than RFI. The radiation is spatially distributed and consists of broadband incoherent microwave emissions. At the AMSR-E low-frequency channels, the atmosphere is relatively transparent, and the polarization and spectral characteristics of the received microwave radiation are dominated by emission and scattering at the surface. Over land, the emission and scattering depend primarily on the water content of the soil, the surface roughness and topography, the surface temperature, and the vegetation cover [10]. The surface brightness temperatures tend to increase with frequency (positive spectral gradient) due to the absorptive effects of water in soil and vegetation that also increase with frequency. However, as the frequency increases, scattering effects from the surface and vegetation also increase, acting as a factor to reduce the brightness temperatures. When volume scattering effects dominate, the brightness temperature spectrum can become flat or even have a negative gradient, i.e., the AMSR-E brightness temperature at 10.7 GHz can be lower than at 6.9 GHz. However, at frequencies below 30 GHz, scattering effects

are usually limited, and such brightness temperature spectral decreases are moderate at most. RFI at C-band is the only possible cause for the brightness temperature at 6.9 GHz to be significantly higher than at 10.7 GHz. Thus, large positive differences obtained by subtracting the 10.7-GHz brightness temperatures from the 6.9-GHz brightness temperatures (negative spectral gradients) can be used to separate RFI at 6.9 GHz from the natural emission background. In this paper, we examined primarily the low-frequency AMSR-E channels (18 GHz and lower) over soil and vegetated land surfaces. It should be noted that scattering signatures can be much stronger for other surfaces such as dry snow, ice, and some desert surfaces. In these cases, the spectral gradient may not be a good indicator of RFI.

IV. RFI IDENTIFICATION

Fig. 1 shows an example of the Level 2A horizontally polarized AMSR-E brightness temperatures at 6.9, 10.7, and 18.7 GHz for a descending pass over the United States. For simplicity, the 6.9-, 10.7-, and 18.7-GHz channels and measurements are designated by 7, 10, and 18 GHz, respectively. Consistent spatial patterns of natural brightness temperature

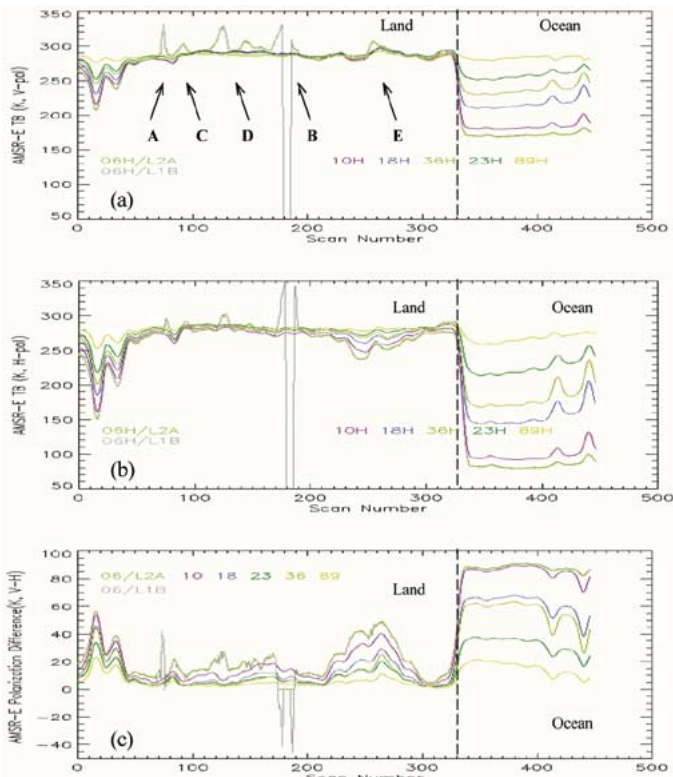


Fig. 2. Subsampled AMSR-E brightness temperatures and polarization differences along descending-pass shown in Fig. 1 (at fixed scan position in swath). Points A, B, C, and D refer to RFI occurrences as described in the text.

variability are visible in all the channels. In the 6.9-GHz image, however, there are several visible “hot spots” where the brightness temperatures far exceed feasible levels for naturally-emitted radiation. These are potential locations of RFI. To examine the RFI and spectral characteristics in detail, we subsampled the AMSR-E data in the along track direction, as indicated by the white line near the center of the swath in Fig. 1. The largest RFI hot spot along this line is located at Denver, CO. Fig. 2 plots sequentially the subsampled brightness temperatures (TBs) at both polarizations V and H, and the polarization difference (TBV – TBH). The sudden drop of the brightness temperature at 6.9 GHz to 0 K is caused by the data processing procedure used by NASDA and RSS. The Level 1B processing resets the brightness temperatures to 0 K when they are larger than a 370-K threshold. The Level 2A processing resets the brightness temperatures to 0 K at a 330-K threshold. These different threshold values contribute to the discrepancy between Level 1B and Level 2A data statistics. Apart from the 6.9-GHz channels, the brightness temperatures in all other channels vary quite smoothly and are well correlated with each other. In the 6.9-GHz channels, several RFI spikes are observed. Where the spike peaks are very high (>330 K), such as at points A, B, and D, there is a positive identification of RFI. The brightness temperatures at C and E are also likely to be RFI-contaminated due to their high spatial frequency and decorrelation with the other channels. At point A, the polarization difference spikes upward, suggesting that the RFI source at this point is mostly vertically polarized. The downward spike of the polarization difference at point B suggests a mostly horizontally polarized RFI source.

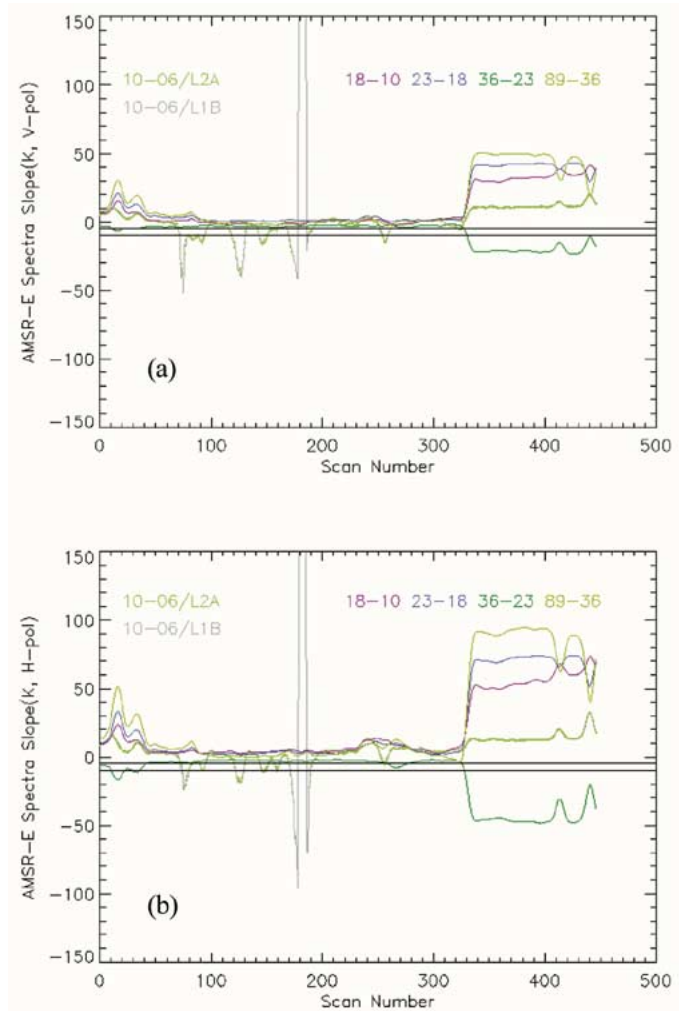


Fig. 3. Subsampled AMSR-E spectral differences for (upper panel) vertical and (lower panel) horizontal polarizations, for same track as Fig. 2.

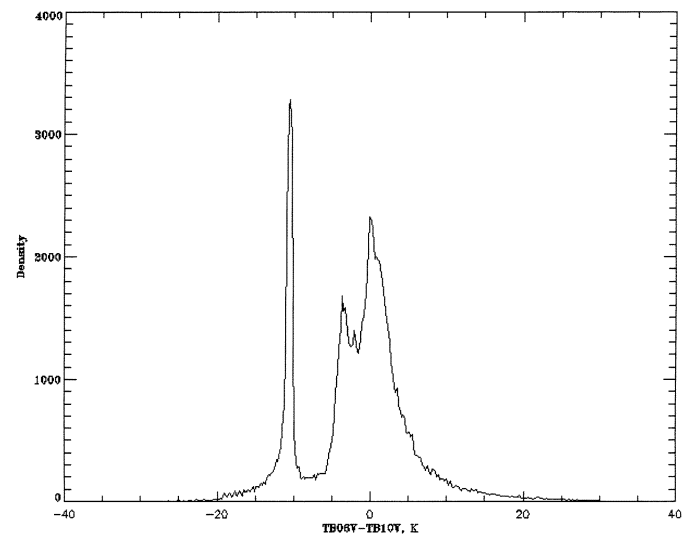


Fig. 4. Histogram of AMSR-E brightness temperature spectral differences (TB7V – TB10V) over the United States.

To examine the spectral signatures, we plotted the spectral differences of the subsampled Level 1B and 2A brightness temperatures in Fig. 3 for both vertical and horizontal polarizations.

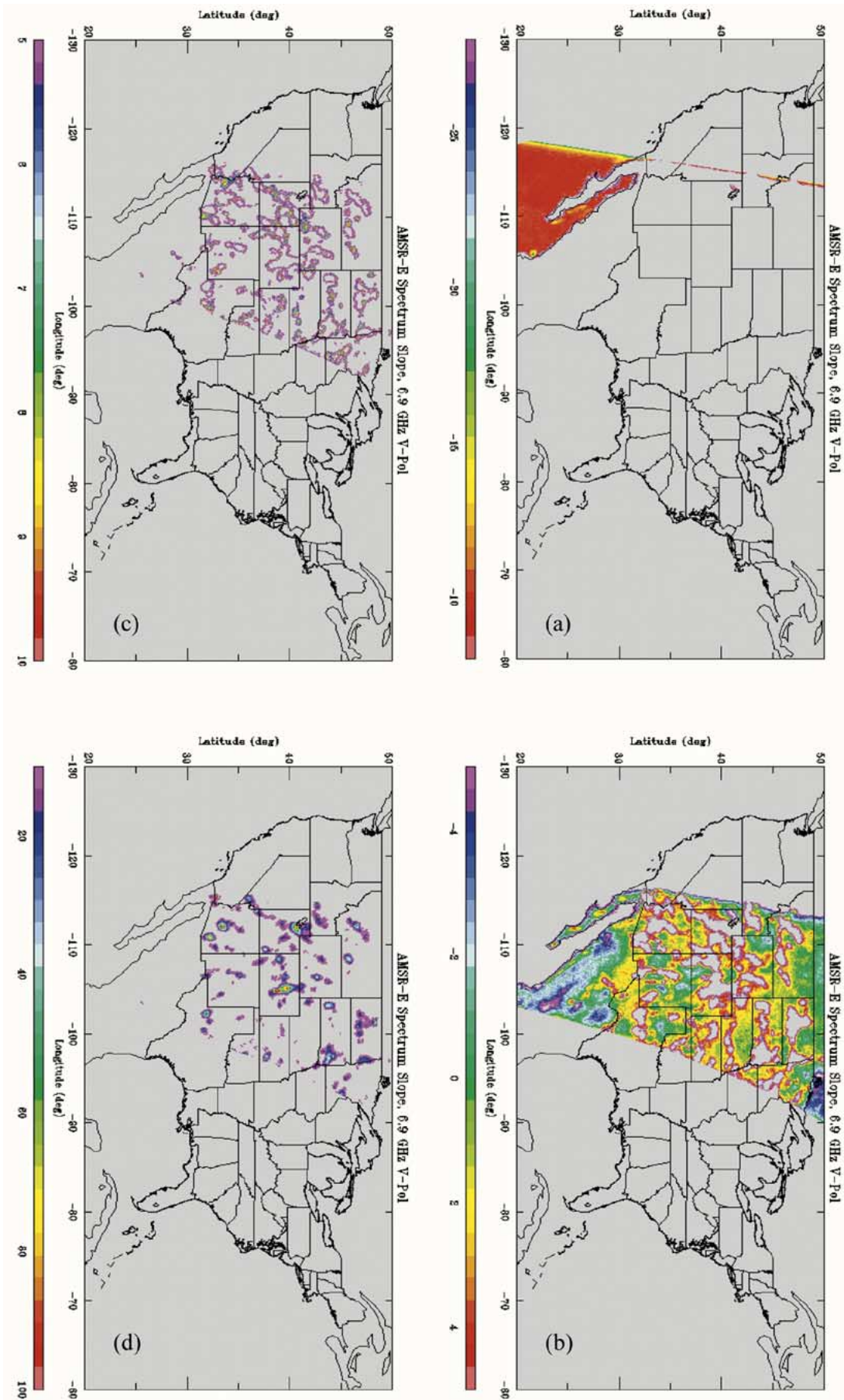


Fig. 5. Classification of AMSR-E measurements based on the RI for one descending pass.

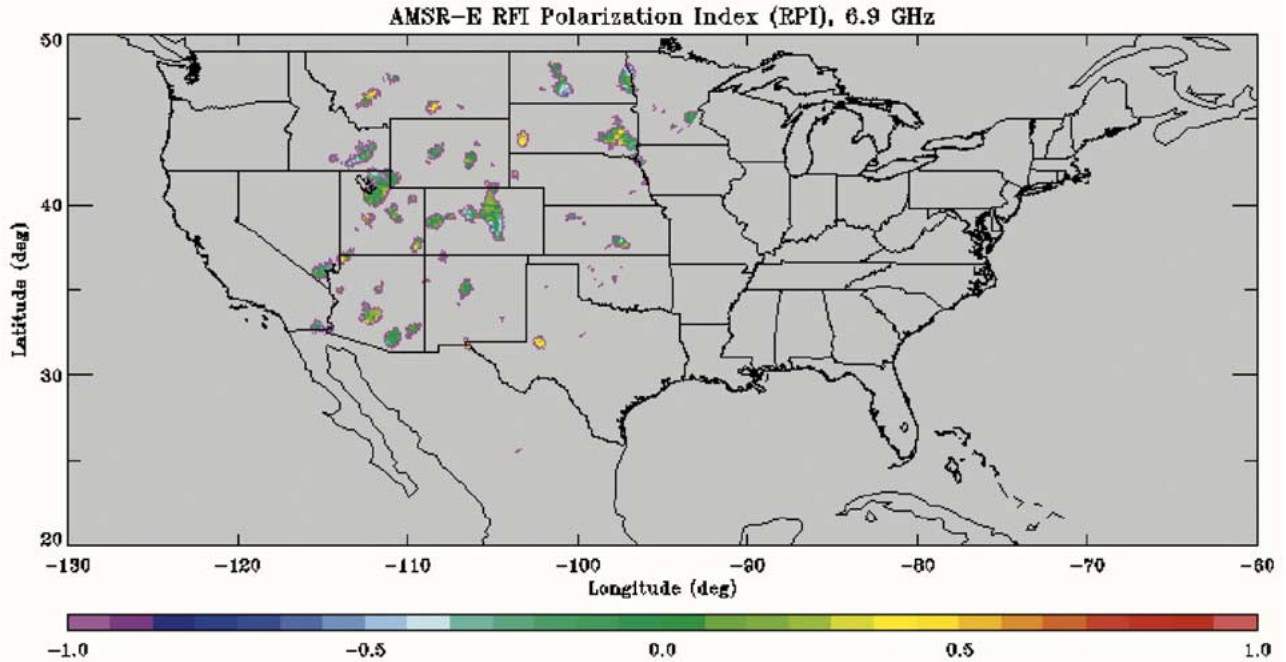


Fig. 6. Map of the RPI over a portion of the United States for one descending pass (same pass as shown in Fig. 5).

When compared with Fig. 2 over the land region, it is clear that the RFI at 6.9 GHz is delineated best by the spectral gradients between 6.9 and 10.7 GHz (i.e., $TB_{10V} - TB_{7V}$ and $TB_{10H} - TB_{7H}$), which can have magnitudes as large as 100 K. For the vertical polarization (top panel), strong RFI can be classed as $(TB_{10V} - TB_{7V}) < -10$ K, and moderate RFI as -10 K $< (TB_{10V} - TB_{7V}) < -5$ K. The horizontal polarization data can be similarly classed. Based on this observation, we have used the negative spectral difference as an RFI Index (RI), i.e., the RI at 6.9 GHz for polarization p is

$$RI_{7p} = TB_{7p} - TB_{10p}. \quad (1)$$

This RI can be used not only to identify the location of RFI but also to quantify its intensity. The larger the RI, the stronger the RFI. Note that a slightly negative RI does not necessarily suggest that the region is RFI-free, since the RFI-free TB_{10p} is often intrinsically higher than the RFI-free TB_{7p} (i.e., negative gradient). Weak RFI could thus increase RI slightly, but not enough to make it positive.

Once a location of RFI has been identified, its polarization characteristics can be calculated using an RFI Polarization Index (RPI), i.e.,

$$RPI = (RIV - RIH)/(RIV + RIH) \quad (2)$$

where $RPI = 1$ for vertically polarized RFI, and $RPI = -1$ for horizontally polarized RFI.

To demonstrate the effectiveness of the spectral gradient in separating RFI from the natural surface background, the RI histogram for the 6.9-GHz vertical polarization ($TB_{7V} - TB_{10V}$) is shown in Fig. 4. There are three peaks near $RI = -12$, -4 , and 1 K. The peak near -12 K represents the ocean signature. The peak near -4 K represents mostly land emission. The third peak

consists of a mixture of land and RFI-contaminated land observations. These can be seen clearly with the RI map in Fig. 5 based on one AMSR-E descending pass, which partitions the brightness temperatures into three RI intervals: 1) $RI < -8$ K contains ocean pixels; 2) -5 K $< RI < 5$ K contains both weak RFI and RFI-free land pixels. Most RFI-free observations are in the negative part of this range; 3) 5 K $< RI < 10$ K contains moderate RFI; 4) $RI > 10$ contains strong RFI. Note that in case 2), it may be quite difficult to separate weak RFI from the natural signal. Fig. 6 shows an example of an RFI polarization index (RPI) map based on one AMSR-E descending pass. It can be seen that the RPI is mostly close to zero, suggesting that the RFI does not appear to favor the vertical or horizontal polarizations, although individual sources should be coherent and polarized. For a few locations in Texas, South Dakota, and Montana, the RFI is predominantly vertically polarized.

We would like to emphasize that the Level 1B and 2A data used here were an experimental release of the AMSR-E products. The brightness temperatures were not fully calibrated at the time of this study. Therefore, the thresholds presented here are likely to change once the AMSR-E data are fully and formally released.

V. RFI SURVEYS OVER NORTH AND CENTRAL AMERICA

A survey of RFI over North and Central America was generated by processing and merging multiple swaths of AMSR-E data for both vertical and horizontal polarizations. The merged ascending-pass swath data for the United States over a three-day period are shown in the two panels of Fig. 7 for V and H polarizations. For reference, in the lower panel the locations of United States cities with populations above 100 000 have been indicated by asterisks (*). It is to be noted that the city locations were extracted from a United Nations database, which contains many errors in city population and city latitude and longitude.

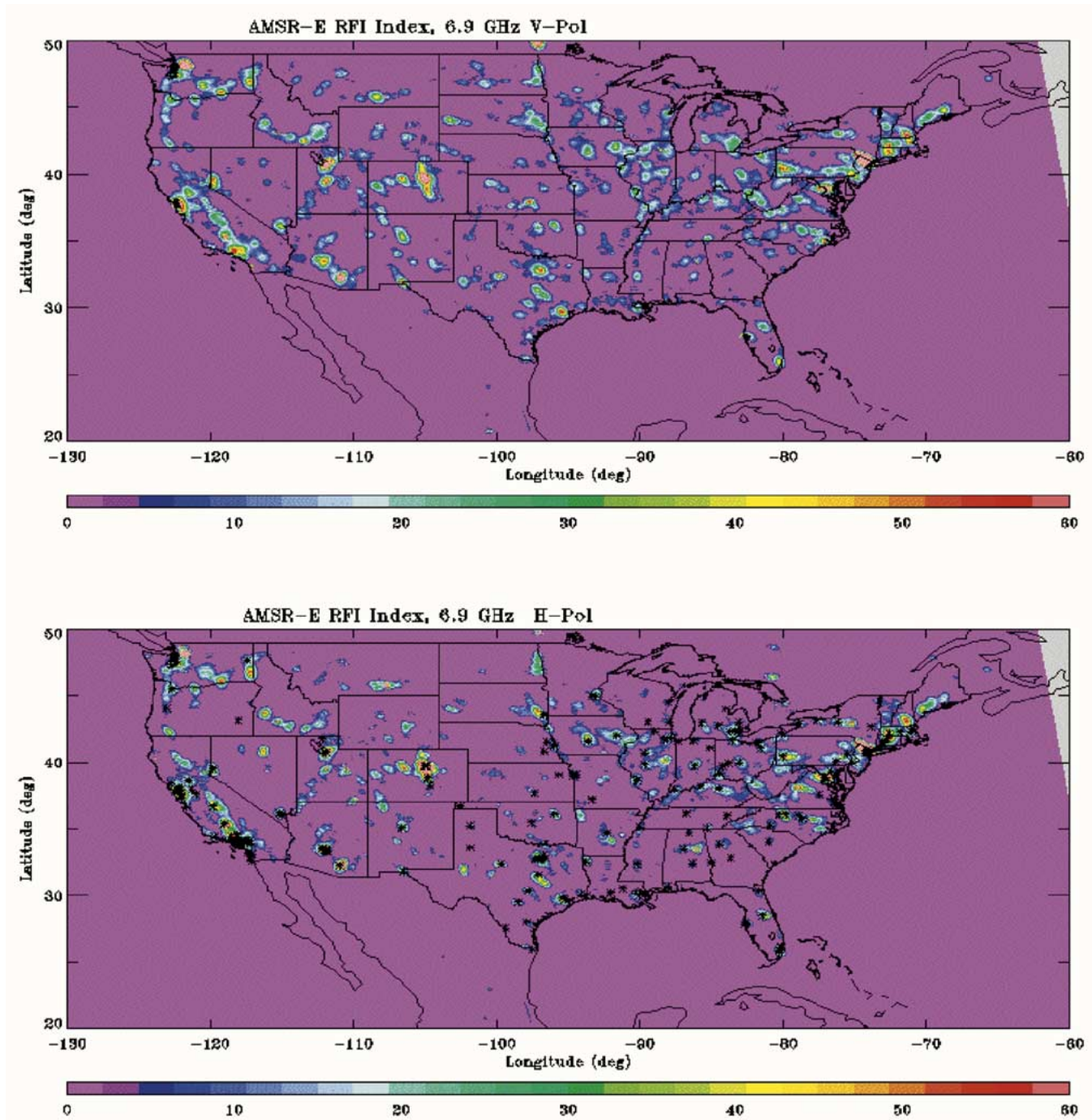


Fig. 7. RI survey maps over the United States using AMSR-E ascending-pass measurements. (Upper panel) Vertical polarization. (Lower panel) Horizontal polarization.

Descending passes are shown in the two panels of Fig. 8. These maps are useful for understanding RFI spatial and temporal variations and investigating the sources and spectra. Several distinct features are visible from the maps.

- 1) In North and Central America, the RFI is confined mostly within the continental United States. There is very little RFI in Canada and Mexico.
- 2) RFI occurs mostly at or near major United States cities or airports, with some exceptions. Some RFI can be distinguished along major highways. The possible RFI sources include, but are not limited to, facilities for cable tele-

vision relay, wireless communication, airport radar, and manufacturing operations, etc.

- 3) Most RFI does not appear to favor vertical or horizontal polarizations, with some exceptions.
- 4) RFI intensities are stronger for ascending (near 1:30 P.M.) than for descending passes (near 1:30 A.M.), which may reflect differences in human activity patterns between day and night. Also, differences in RFI between ascending and descending passes may be due to differences in the AMSR-E antenna azimuth viewing direction of RFI sources.

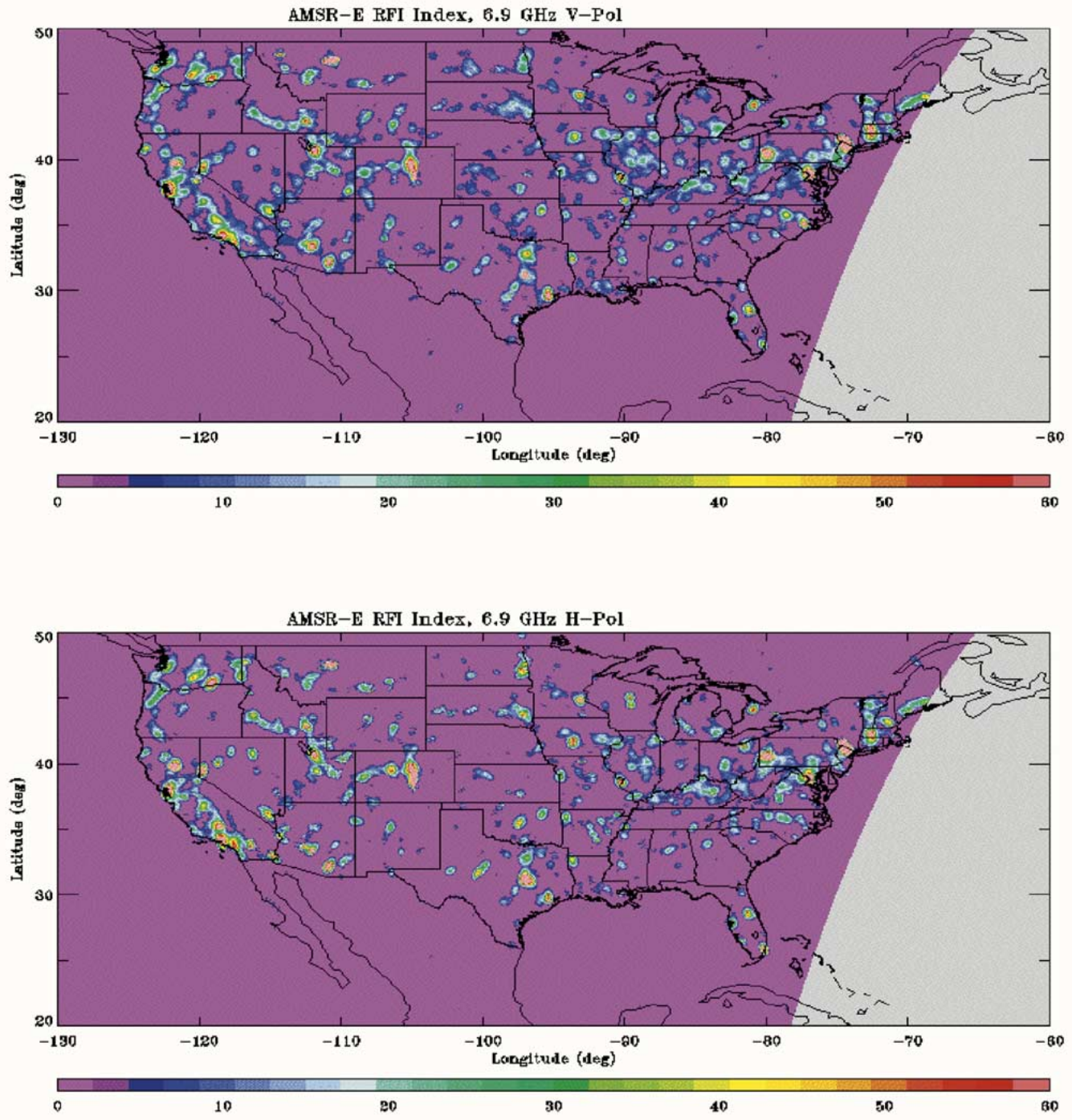


Fig. 8. Same as Fig. 7 but for descending-pass measurements.

More detailed regional maps were generated to focus on specific AMSR-E targets of interest, in particular the planned United States soil moisture validation sites [1]. Fig. 9 shows RFI maps for the regions of (a) Iowa, (b) Oklahoma, and (c) Alabama/Georgia. Cities with populations above 100 000 are indicated by asterisks. In Fig. 9(a), there is widespread RFI evident in the neighborhoods of Des Moines, Cedar Rapids, and Sioux Falls, though not centered directly on those cities. Surprisingly, there is no RFI near Madison and Lincoln despite the sizeable population and urbanization of these cities. Addi-

tional investigations need to be undertaken using ground-based RFI detectors to locate and characterize the specific sources of the RFI.

VI. INNOVATIVE CONCEPT FOR RADIOMETER SYSTEM DESIGN AND RFI SUPPRESSION TECHNIQUE

The RFI contamination problem will compromise the science objectives of AMSR-E that use the 6.9-GHz channels over land, as well as its sister instrument, AMSR, on the Japanese ADEOS-II satellite. If not properly corrected, the science value

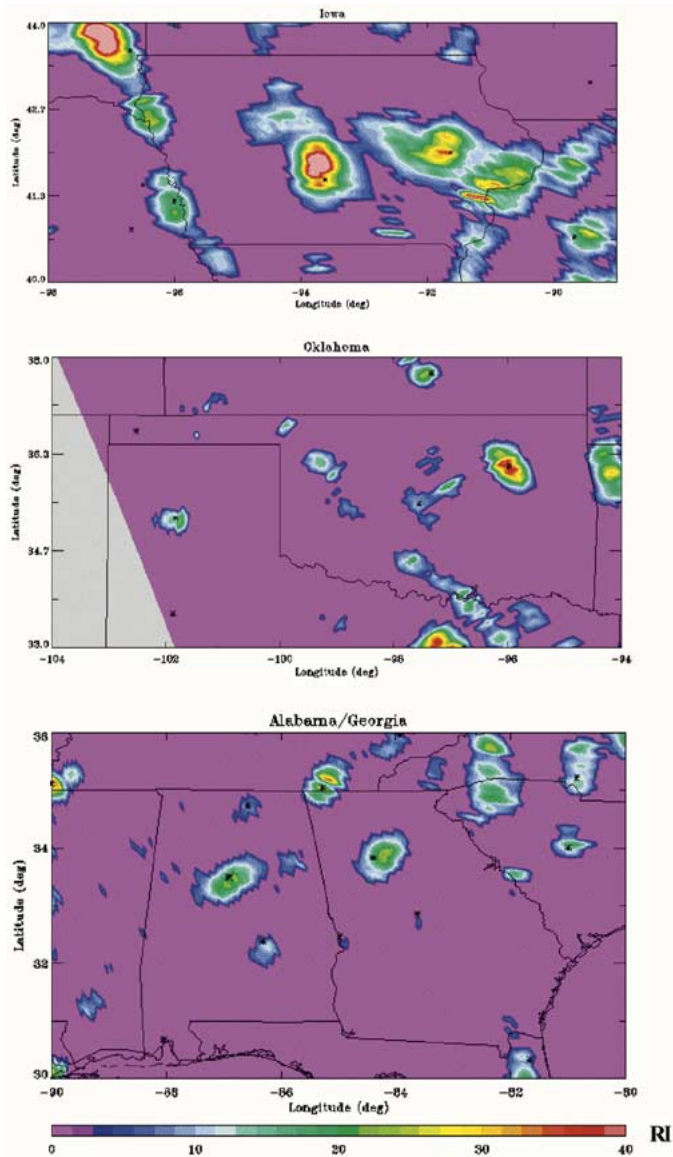


Fig. 9. RI maps of regional areas in the United States centered in (a) Iowa, (b) Oklahoma, and (c) Alabama/Georgia.

of spaceborne radiometers for many other missions, including the Navy WindSat and NPOESS CMIS, will also be reduced. All of these missions have included C-band channels to enhance their land and ocean surface sensing capabilities, especially the soil moisture monitoring capability from space, which is one of the top science priorities for NASA and NPOESS for the next decade. To preserve these science capabilities, some RFI mitigation approaches must be developed.

Although RFI contamination is an emerging challenge for spaceborne radiometry, it has been recognized as a problem for active sensors for many years. Over the last decade, many RFI suppression technologies have been developed successfully for ultrawideband radar systems [11], [12]. Those technologies can be adopted for radiometry with certain modifications to the radiometer system design, which can be understood through following comparisons between active and passive sensors.

Active sensors transmit coherent signals and perform coherent processing on the received backscattering signals, which

have both coherent and incoherent components. The RFI is imposed on the coherent component with different spectral signatures. Because coherent detection is used in active sensor, we can transform the received signals into the frequency domain and filter out the RFI coherently and adaptively by seeking zero correlation between RFI and natural targets while minimizing the RFI prediction error.

In a conventional radiometer, a square-law detector is often used to measure the total power received, which is an irreversible process in which the natural radiation and RFI are summed together and cannot be separated. Furthermore, because the phase information is discarded at the very beginning of data processing, no spectral information can be collected, and therefore RFI cannot be removed coherently in the frequency domain. However, an RFI removal capability can be added by replacing the square-law detector with a high-performance A/D converter and an onboard data processor. With the emergence of wideband, high dynamic range A/D converters, it is straightforward to implement such a new concept for radiometry [13]. Once the spectra of the received signals are sampled coherently, the active RFI suppression technique can be adopted to remove the coherent part of the spectra from the incoherent thermal noise (brightness temperature) background. The sampled spectra are also useful in studying the RFI sources and their signatures, which is essential in developing RFI suppression algorithms. In addition, RFI suppression processing can be performed onboard, in real-time and updated throughout the mission using the field-programmable gate-array-based programmable processing technology.

VII. DISCUSSION

In this paper, we have examined only RFI over land. This does not necessarily suggest that there is no RFI over ocean regions, only that our first priority has been to examine the distribution of major RFI sources over land and their impact for land remote sensing. Also, we have analyzed primarily data over the United States since our preliminary survey indicated that this was the region with the most widespread and severe RFI. In subsequent studies, the RFI over other land regions and ocean regions will be examined also.

ACKNOWLEDGMENT

The AMSR-E data are made available as part of the NASDA/NASA AMSR-E team activities and were accessed through the AMSR-E SIPS facility at NASA/MSFC.

REFERENCES

- [1] T. Kawanishi, T. Sezai, Y. Ito, K. Imaoka, T. Takeshima, Y. Ishido, A. Shibata, M. Miura, H. Inahata, and R. W. Spencer, "The Advanced Microwave Scanning Radiometer for the Earth Observing System (AMSR-E), NASA's contribution to the EOS for global energy and water cycle studies," *IEEE Trans. Geosci. Remote Sensing*, vol. 41, pp. 184–194, Feb. 2003.
- [2] K. Imaoka, T. Sezai, T. Takeshima, T. Kawanishi, and A. Shibata, "Instrument characteristics and calibration of AMSR and AMSR-E," in *Proc. IGARSS*, Toronto, ON, Canada, June 2002.
- [3] P. W. Gaiser and K. M. St. Germain, "Spaceborne polarimetric microwave radiometry and the Coriolis WindSat system," in *Proc. IEEE Aerospace Conf.*, vol. 5, 2000, pp. 159–164.

- [4] D. B. Kunkke, N. S. Chauhan, and J. J. Jewell, "Phase one development of the NPOESS Conical-Scanning Microwave Imager/Sounder," in *Proc. IGARSS*, Toronto, ON, Canada, June 2002.
- [5] E. Njoku, J. M. Stacey, and F. T. Barath, "The SEASAT Scanning Multichannel Microwave Radiometer (SMMR): Instrument description and performance," *IEEE J. Oceanic Eng.*, vol. 5, pp. 100–115, 1980.
- [6] J. P. Hollinger, J. L. Peirce, and G. A. Poe, "SSM/I instrument evaluation," *IEEE Trans. Geosci. Remote Sensing*, vol. 28, pp. 781–790, Sept. 1990.
- [7] C. Kummerow, J. Simpson, O. Thiele, W. Barnes, A. T. C. Chang, E. Stocker, R. F. Adler, A. Hou, R. Kakar, F. Wentz, P. Ashcroft, T. Kozu, Y. Hong, K. Okamoto, T. Iguchi, H. Kuroiwa, E. Im, Z. Haddad, G. Huffman, B. Ferrier, W. S. Olson, E. Zipser, E. A. Smith, T. Wilheit, G. North, T. Krishnamurti, and K. Nakamura, "The status of the Tropical Rainfall Measuring Mission (TRMM) after two years in orbit," *J. Appl. Meteorol.*, vol. 39, no. 12, pp. 1965–1982, 2000.
- [8] P. Ashcroft and F. Wentz. (2000, Nov.) Algorithm theoretical basis document, AMSR Level 2A Algorithm, Remote Sensing Systems, Santa Rosa, CA. [Online] RSS Tech. Report 121 599B-1
- [9] ITU, "Radio Regulations," Int. Telecommun. Union, Geneva, Switzerland, 2001.
- [10] E. G. Njoku and L. Li, "Retrieval of land surface parameters using passive microwave measurements at 6–18 GHz," *IEEE Trans. Geosci. Remote Sensing*, vol. 37, pp. 79–93, Jan. 1999.
- [11] T. Miller, L. Potter, and J. McCorkle, "RFI suppression for ultra wideband radar," *IEEE Trans. Aerosp. Electron. Syst.*, vol. 33, pp. 1142–1156, Oct. 1997.
- [12] C. Le, S. Hensley, and E. Chapin, "Removal of RFI in wideband radar," in *Proc. IGARSS*, July 1998, pp. 2032–2034.
- [13] S. W. Ellingson, G. A. Hampson, and J. T. Johnson, "Design of an L-band microwave radiometer with active mitigation of interference," in *Proc. NASA Earth Science Technology Conf.*, July 2003.



Eni G. Njoku (M'77–SM'83–F'95) received the B.A. degree in natural and electrical sciences from Cambridge University, Cambridge, U.K., in 1972, and the M.S. and Ph.D. degrees in electrical engineering from the Massachusetts Institute of Technology, Cambridge, in 1974 and 1976.

From 1976 to 1977, he was a National Research Council Resident Research Associate. In 1977, he joined the Jet Propulsion Laboratory (JPL), Pasadena, CA, where he is currently a Principal Scientist. His primary interests are in the use of passive and active microwave remote sensing for hydrology and climate applications. His research involves studies of microwave interactions with land surfaces and retrieval algorithm development. He is currently a member of the Aqua Advanced Microwave Scanning Radiometer science team. From 1986 to 1990, he served as Discipline Scientist for Ocean and Earth Science Data Systems at NASA Headquarters, Washington, DC, and from 1993 to 1994, he was Manager of the Geology and Planetology Section at JPL. During the 2001–2002 academic year, he was on leave as a Visiting Professor at the Massachusetts Institute of Technology. He was Principal Investigator for the IIP OSIRIS technology study and is currently Project Scientist for the Earth System Science Pathfinder HYDROS mission.

Dr. Njoku is a member of the American Meteorological Society, the American Geophysical Union, the American Association for the Advancement of Science, Commission F of the International Union of Radio Science, and Sigma Xi. He has served as an Associate Editor of the *IEEE TRANSACTIONS ON GEOSCIENCE AND REMOTE SENSING* (1985–1988) and was the Technical Program Chairman for IGARSS'94 held in Pasadena, CA. He has been a recipient of NASA Group Achievement Awards in 1980, 1982, and 1985, and he was awarded the NASA Exceptional Service Medal in 1985.

Eastwood Im (S'81–M'85–SM'01) received the B.S., M.S., and Ph.D. degrees in electrical engineering from the University of Illinois, Urbana, in 1981, 1982, and 1985, respectively.

He has been with the Jet Propulsion Laboratory (JPL), California Institute of Technology, Pasadena, since 1986. His research interests are in the areas of spaceborne meteorological radar science and remote sensing, and advanced radar system and technology studies. In particular, he has developed radar algorithms for the retrievals of precipitation intensity and surface topography, and the two-color laser altimetry algorithms for measuring surface pressure and tectonic motions. He has been involved in several design studies on spaceborne earth remote sensing radars, including precipitation radars, altimeters, and millimeter-wave cloud radars. He is currently the Radar Instrument Manager of the NASA ESSP CloudSat Mission and the Supervisor of the Atmospheric Radar Science and Engineering program at JPL. He has been a member of the Tropical Rainfall Measuring Mission (TRMM) Science Team and a Principal Investigator in TRMM radar rain profiling algorithms and TRMM radar calibration, and the Principal Investigator of the IIP Second-Generation Precipitation Radar (PR-2) technology study. He has also been a Co-Investigator of several other NASA research studies. Currently, he is the Principal Investigator in four NASA earth science research studies: the IIP dual-frequency wide-swath scanning rain radar antenna study, the IIP NEXRAD-in-Space radar study, the CAMEX-4 airborne radar's rainfall observation experiment, and the validation of the EOS AQUA AMSR-E's rainfall measurements. He is also the Co-Investigator on NASA ESE AIST's (Advanced Information System Technology program) advanced spaceborne rain radar processor and is the Guest-Investigator on the radar study of Titan's atmospheric methane precipitation in NASA's Cassini Mission. He has been a Member of a science steering group on the NASA Global Precipitation Mission since its inception, focusing particularly in the areas of radar performance and technology development and infusion.

Dr. Im is a Senior Member of the Institute of Electrical and Electronics Engineers, and a member of American Meteorological Society, Eta Kappa Nu, and Tau Beta Pi. He received the University of Illinois Graduate College Dissertation Research Grant in 1984; the GT&E Fellowship in 1984; Kemper Fellowship and Exxon Fellowship in 1985, NASA Group Achievement Awards in 1998 and 2002, JPL Award of Excellence in 2002, and eight NASA New Technology Awards. Dr. Im served as the Associate Editor of the *AMS Journal of Atmospheric and Oceanic Technology* in 1999–2000, and as a member of the Technical Program Committee and a Technical Session Chair/Co-Chair of the IGARSS symposia between 1999 and 2003. He has published over 130 articles in refereed journals and conference proceedings, and 11 technical reports.

Li Li (M'96) received the M.S. degree from Beijing University of Posts and Telecommunications, Beijing, China, and the Ph.D. degree from the University of Washington, Seattle, in 1987 and 1995, respectively, both in electrical engineering.

He is currently a Senior Scientist with the Jet Propulsion Laboratory, California Institute of Technology, Pasadena. He was a Student Visitor from 1993–1995 at the National Center for Atmospheric Research, Boulder, CO. From 1995 to 1997, he was with the Caelum Research Corporation, Rockville, MD, working at the Office of Research and Applications, National Environmental Satellite, Data and Information Service, National Oceanic and Atmospheric Administration (NOAA/NESDIS), Camp Springs, MD, where he conducted research in the area of polarimetric microwave radiometry, especially for the concept study of ocean surface wind vector sensing. He has been with the Jet Propulsion Laboratory since 1997 and has participated in several NASA projects, including the land algorithm development for Aqua Advanced Microwave Scanning Radiometer (AMSR-E), sensor calibration and Level 1B processing for CloudSat Cloud Profiling Radar (CPR), TRMM cross-sensor calibration and data analysis, second-generation precipitation radar data calibration and analysis, and ocean surface latent heat flux studies. His current research interests include passive and active remote sensing of land and ocean surfaces, as well as precipitation profiling for applications related to climate study and monitoring.

Dr. Li is a member of the American Geophysical Union, the IEEE Geoscience and Remote Sensing Society, and Eta Kappa Nu. He has been a recipient of the NCAR/RAP Fellowship 1993–1995 and the NASA Group Achievement Award and JPL Technical Excellence Award, both in 2002.

Paul S. Chang (S'93–M'95–SM'03) received the B.S. degree in electrical engineering from Union College, Schenectady, NY, in 1988, and the Ph.D. degree in electrical engineering from the University of Massachusetts, Amherst, in 1994.

Since 1994, he has been with the Office of Research and Applications, National Environmental Satellite, Data and Information Service, National Oceanic and Atmospheric Administration, Camp Springs, MD. His primary interests have been active and passive microwave remote sensing of the ocean surface, with emphasis on the retrieval of the ocean surface wind vector. He is currently involved in the calibration and validation activities of WindSat (polarimetric radiometer) on Coriolis and SeaWinds (ku-band scatterometer) on ADEOS-II. He is also leading an effort to demonstrate and quantify the impacts of satellite remotely sensed ocean vector wind data on operational marine short-term forecasting and warnings.



Karen St. Germain (S'88–M'91–SM'03) received the B.S. degree in electrical engineering from Union College, Schenectady, NY, in 1987, and the Ph.D. degree from the University of Massachusetts, Amherst, in 1993.

From 1987 to 1993, she was a Research Assistant in the Microwave Remote Sensing Laboratory, University of Massachusetts, where her doctoral research focused on passive microwave remote sensing of oceans and ice. In 1993, she joined the Faculty of the Department of Electrical Engineering,

University of Nebraska, Lincoln. While at the University of Nebraska, she taught courses in electromagnetics, signal processing, and radar system design, and expanded her research interests to include passive and active remote sensing of vegetation and soil moisture. In 1996, she left the University of Nebraska to take a position at the Naval Research Laboratory, Washington DC, where she is currently involved in remote sensing system development, spaceborne demonstration of remote sensing concepts, instrument calibration, radiative transfer theory, and algorithm development.

Dr. St. Germain has been a member of the IEEE Geoscience and Remote Sensing Society (GRSS) since 1988. She served as an Associate Editor of the IEEE GRSS Newsletter from 1994 to 1996 and was elected to the GRSS AdCom in 1997. She served as the Membership Chairman from 1997 to 1998 and has served as the Vice President for Meetings and Symposia from 1998 to 2003. She is currently Vice President of Operations and Finance. She was Co-Chairman of the Technical Program for IGARSS 2000 and is a member of Eta Kappa Nu and Tau Beta Pi. She currently serves on the U.S. National Research Council's Committee on Radio Frequencies (CORF).